Cui *et al. BMC Plant Biology* (2025) 25:665
https://doi.org/10.1186/s12870-025-06709-1

BMC Plant Biology

RESEARCH Open Access

Integration of lipidomics and widely targeted metabolomics provides a comprehensive metabolic landscape of *Poa pratensis* under cadmium stress

Ting Cui[1], Yong Wang[1], Kuiju Niu[1], Chunxu Zhao[1] and Huiling Ma[1*]

Abstract

Background Soil cadmium (Cd) contamination poses significant environmental challenges globally. Kentucky bluegrass is considered a viable plant for remediating Cd-contaminated soils due to its high tolerance to Cd and accumulation capacity. Yet, the complete metabolic landscape underlying Cd detoxification mechanisms of Kentucky bluegrass remains incompletely understood.

Results Here, widely targeted metabolomics was used to identify key metabolites of Kentucky bluegrass that were responsive to Cd stress in comparisons between Cd-resistant (M) and sensitive (R) varieties. Moreover, lipidomics analyses were used to assess the content, composition, and saturation levels of lipid molecular species. The M variety exhibited higher levels of free amino acids, saccharides, and flavonoids (flavones, flavonols, isoflavones, and flavanones) after Cd stress that likely enhance its tolerance to Cd stress. Within the M variety, 183 lipid species (81%) were less abundant after Cd stress, representing a much larger number than the 81 lipid species (41.54%) similarly less abundant in the R variety. The lipid species with increased abundances primarily comprised diacylglycerols, monogalactosyldiacylglycerol, phosphatidylcholine, triacylglycerol, and lysophosphatidylcholine that exhibited higher saturation levels. Conversely, the lipid species with decreased abundances largely comprised those with shorter acyl chains including free fatty acids, phosphatidic acid, and lysophosphatidic acid, as well as those with higher unsaturation levels, including phosphatidylglycerol, diacylglycerol, triacylglycerol, phosphatidylcholine, and lysophosphatidylcholine. The elongation of these lipid acyl chains under Cd stress contributes to the increased membrane thickness and rigidity in Kentucky bluegrass, resulting from the dense packing of hydrophobic tails and enhanced lipid-lipid interactions. The changes in these metabolites and lipids may play a significant role in enhancing Cd tolerance, distribution, and accumulation in Kentucky bluegrass.

Conclusion The results of this study provide a comprehensive metabolite profile for Kentucky bluegrass in response to Cd stress, elucidating the key metabolite characteristics essential for Cd detoxification under Cd-induced stress. Furthermore, the results provide insights into the metabolic regulation of metabolites and lipid homeostasis that contribute to enhanced Cd tolerance in Kentucky bluegrass.

*Correspondence:
Huiling Ma
mahl@gsau.edu.cn

Full list of author information is available at the end of the article

Keywords Kentucky bluegrass, Cadmium toxicity, Lipidomic, Widely targeted metabolomic

Introduction

Cadmium (Cd) is among the most serious heavy metal soil pollutants in China [1, 2]. By 2019, most soil around non-ferrous smelteries in China exhibited Cd levels surpassing severe pollution thresholds [3]. Mining operations are noteworthy contributors to Cd emissions into environments. A marked rise in Cd emissions has been attributed to Chinese mining activities during the period from 1990 to 2015 [4]. Cd from mining areas and non-ferrous metal smelters can enter agricultural ecosystems through atmospheric deposition and rainwater flows [2]. Importantly, crops containing enriched levels of Cd, when ingested by humans and other animals, have the potential to cause renal and pulmonary ailments [1]. Therefore, remediating Cd-contaminated soils around mining sites and non-ferrous metal smelters helps prevent further spread of Cd pollution from origin points.

Phytoremediation strategies are environmentally friendly and plant-based, playing critical roles in mitigating Cd toxicity [5–7]. Nevertheless, prolonged Cd accumulation usually inhibits plant growth [8], triggers oxidative stress [9], causes leaf chlorosis [7], and can ultimately lead to plant death [10, 11]. Seven Cd hyperaccumulator plant species have previously been identified [12]. However, low tolerance to Cd stress, limited biomass, and the slow growth rates of these plants restrict their use in remediation of Cd-contaminated soils. Kentucky bluegrass is a cool-season turfgrass widely distributed globally in temperate regions [13, 14]. Kentucky bluegrass is considered a promising candidate for remediation of Cd-contaminated soil due to its significant biomass accumulation and high Cd tolerance [6, 15, 16]. A previous study revealed that Kentucky bluegrass growth was unaffected by treatment with 40 mg Cd kg^{-1} treatment, while growth of the hyperaccumulator plant *Solanum nigrum* was significantly suppressed at the same Cd concentration [17]. Moreover, the aboveground tissues of Kentucky bluegrass accumulated 17.1-fold higher Cd than *Solanum nigrum* under treatment with 40 mg Cd kg^{-1} after 9 weeks of exposure [17]. Kentucky bluegrass consequently carries significant potential value for remediating Cd-contaminated soils.

Enhancing plant tolerance to Cd during phytoremediation of Cd-contaminated soils helps maintain long-term Cd uptake by plants and improves phytoremediation efficiency [6]. Previously, various conserved mechanisms in plants have been identified that enable Cd detoxification, including via use of cell wall polysaccharides for Cd immobilization [18], metal ligands for Cd chelation [19], cell wall lignification [20], and vacuolar Cd sequestration [9]. These mechanisms have been applied in the breeding of Cd-safe crops and the cultivation of plants for remediating Cd-contaminated soils [9, 21–23]. Further, key metabolites, including organic acids [15], hormones [8], signaling molecules [24], and sugars [25, 26] have been used as exogenous substances to enhance plant Cd tolerance and regulate Cd uptake and distribution in plants. However, technological considerations have impeded a thorough evaluation of important Cd-stress related metabolites at the molecular level, in addition to detoxification pathways of plants that respond to Cd stress, thereby hampering enhanced application of plant remediation technologies when restoring Cd-contaminated soils.

Numerous studies have demonstrated a significant role for cell walls in Cd detoxification and immobilization [18, 22, 27–29]. Plant plasma membranes are also important targets of Cd stress [30]. The production of signaling lipids during stressful conditions plays an important role in activating subsequent signaling pathways that then elicit physiological responses [31]. Metabolomics can be used to identify primarily hydrophilic polar compounds, while lipidomics can primarily be used to identify hydrophobic nonpolar compounds [32]. Unlike conventional untargeted metabolomics studies, widely-targeted metabolomics achieve the broad scope of untargeted metabolomics, with the accuracy of targeted metabolomics, thereby providing a powerful method to identify specific metabolites in plants [33]. Further, the integration of widely-targeted metabolomics and lipidomics provides information about detailed metabolic landscapes and facilitates thorough network analysis that can identify critical metabolic factors in plants under Cd stress. Consequently, these integrated methods can enhance our understanding of the interconnectedness between lipids and other metabolites in response to Cd stress [32, 34, 35]. Therefore, integrating widely-targeted metabolomics and lipidomics enables comprehensive detection of polar and nonpolar compounds responding to Cd stress in Kentucky bluegrass, and provides novel candidate metabolites with key metabolic pathways to enhance Cd tolerance and accumulation in this grass species. Here, a comprehensive metabolomic landscape of Kentucky bluegrass during Cd stress was evaluated by integrating lipidomic and widely targeted metabolomics analyses. In addition, a comparison of the metabolite profiles of Cd-tolerant and Cd-sensitive Kentucky bluegrass cultivars was conducted to identify important metabolic pathways that enhance Kentucky bluegrass tolerance to Cd stress. The study provides new insights into the functional metabolites that enhance the tolerance of Kentucky bluegrass to Cd stress. Indeed, some

of these metabolites may serve as compounds that could be potentially applied during plant remediation in Cd-contaminated soils that would help increase tolerance of Kentucky bluegrass to Cd stress.

Materials and methods

Cultivation of Kentucky bluegrass

Previously, a Cd-tolerant Kentucky bluegrass variety, Midnight (M), and a Cd-sensitive variety, Rugby II (R), were identified from a pool of 12 Kentucky bluegrass varieties by assessing variation in germination, photosynthesis, growth, and physiological traits under Cd stress [16, 36]. The present study further investigated the mechanisms that enhance Cd tolerance in Kentucky bluegrass using the Cd-tolerant M and Cd-sensitive R varieties. The Kentucky bluegrass seeds for the M and R varieties were provided by Clover Ecological Technology Co., LTD (Beijing, China).

Seeds of Kentucky bluegrass varieties M and R were evenly sown into pots (30 cm × 20 cm × 20 cm) filled with vermiculite that were covered with a 1 cm layer of vermiculite and sprayed daily with distilled water to keep the vermiculite moist. After germination of the M and R seeds, they were irrigated with Hoagland nutrient solution [37]. Seedlings were cultivated in an artificial climate incubator. Cultivation temperature was maintained at 25/20°C (light/dark) with a light intensity of 360 μmol m^{-2} s^{-1}, a photoperiod of 16 h light/8 h dark, and a relative humidity of 65% [8]. After 1 month of pre-cultivation, M and R seedlings were transplanted into opaque hydroponic containers (12 cm length × 8 cm width × 11 cm height). The lids of the hydroponic containers were equipped with 6 holes, each containing 3 Kentucky bluegrass plants. The plants were secured at the base of the shoots using sponges. Cd stress treatment was initiated after an additional 15 days of cultivation with Hoagland nutrient solution in the hydroponic containers.

Cd treatment

The M and R varieties were divided into control (CK) and treatment (Cd) groups. Each treatment comprised 6 individual hydroponic boxes as biological replicates. The control groups for the M and R varieties were cultivated with Hoagland nutrient solution, while the treatment groups were exposed to Cd stress using 600 μM of $CdCl_2{\cdot}2.5H_2O$ in the same Hoagland nutrient solution. After 3 days of Cd treatment, widely-targeted metabolomic and lipidomic analysis were conducted using the roots of M and R varieties after Cd and Cd-free conditions. Each treatment group comprised three biological replicates.

Sample preparation and metabolome extractions

Fresh root samples of Kentucky bluegrass (0.2 g) were freeze-dried using a lyophilizer (Scientz-100 F, Ningbo, China) and subsequently homogenized into a uniform paste using liquid nitrogen. Metabolites from the homogenized samples were extracted using 1.2 mL of pre-cooled (– 20 °C) 70% methanolic aqueous internal standard extract. Extraction lasted for 30 min, during which the samples were vortexed every 5 min for 30 s each time. The samples were then centrifuged at 12,000 rpm for 3 min, followed by collection of supernatants and filtering through a 0.22 μm microporous membrane.

Metabolite analysis with UPLC-ESI-MS/MS

Metabolites in the filtrates discussed above were identified using an ultra-performance liquid chromatography-electrospray ionization-tandem mass spectrometry (UPLC-ESI-MS/MS) system (UPLC, ExionLC™ AD, https://sciex.com.cn/, Framingham, USA) and a tan dem mass spectrometry system (https://sciex.com.cn/) [38, 39]. The UPLC system was equipped with an Agilent SB-C18 column (1.8 μm, 2.1 mm × 100 mm) and used a mobile phase comprising solvent A (pure water with 0.1% formic acid) and solvent B (acetonitrile with 0.1% formic acid). Sample measurements were conducted using a gradient starting with 95% of solvent A and 5% of solvent B. Over 9 min, a linear progression to 5% of solvent A and 95% of solvent B, followed by a 1 min retention at 5% of solvent A and 95% of solvent B. The composition was then changed to 95% solvent A and 5.0% of solvent B within 1.1 min and maintained for 2.9 min. The flow rate was set at 0.35 mL/min, the column oven temperature at 40 °C, and the injection volume at 2 μL. The effluent was directed to an ESI-triple quadrupole-linear ion trap (QTRAP)-MS system.

ESI source operation parameters included a source temperature set to 500 °C, ion spray voltage in the positive ion mode set to 5,500 V, and set to – 4,500 V in the negative ion mode. The gas settings for ion source gas I, gas II, and curtain gas were maintained at 50, 60, and 25 psi, respectively. The collision-induced ionization parameter was set to high. Multiple reaction monitoring experiments with collision gas (nitrogen) set to medium were used to acquire QQQ scans. The declustering potential and collision energy for individual multiple reaction monitoring transitions were optimized, followed by a specific set of monitored transitions for each period based on eluted metabolites.

Identification and quantification of metabolites

Qualitative analysis of the detected metabolites was conducted based on the Metware database (Metware Biotechnology Co., Ltd, Wuhan, Hubei, China) [40]. The chromatographic peaks detected for each metabolite in samples were corrected based on retention time and peak information to enable comparison of abundances of each metabolite among different samples. The corrections

ensured accurate qualitative and quantitative analyses [41].

Sample quality control and differential metabolite analyses

Quality control (QC) samples were prepared by mixing sample extracts to assess the reproducibility of sample analyses when using the same processing conditions. Principal component analysis (PCA) was conducted on all samples, including the QC samples, to evaluate overall metabolite differences between sample groups and within-group variation [42]. Metabolite profiles were also analyzed using Partial Least Squares-Discriminant Analysis (PLS-DA) combined with orthogonal signal correction (OSC) to more comprehensively investigate differences among treatment groups using multivariate statistical analysis [43]. Differentially expressed metabolites (DEMs) were selected by integrating variable importance in projection (VIP) values obtained from the OPLS-DA model with fold-change (FC) values derived from univariate analysis. Metabolites were considered as DEMs between different comparison groups if they had VIP > 1 and FC ≥ 2 or FC ≤ 0.5. DEMs were further annotated against the Kyoto Encyclopedia of Genes and Genomes (KEGG) database to investigate metabolic pathways involved in responses to Cd stress [44].

Sample preparation and lipidome extractions

Freeze-dried samples were prepared as indicated in Sect. 2.1. A total of 0.02 g of freeze-dried root samples were extracted in 1 mL of extraction solvent (MTBE: MeOH = 3:1, v/v) that was supplemented with an internal standard mixture. After shaking at 2,500 rpm for 15 min, 300 µL of ultrapure water was added, followed by 1 min of shaking and then incubation at 4 °C for 10 min. The mixtures were centrifuged at 12,000 rpm for 10 min, followed by collection of 200 µL supernatant. The supernatant was subsequently concentrated at 20 °C for 2 h until completely dry. The dried extracts were dissolved in 200 µL of the reconstituted solution (ACN: IPA = 1:1, v/v) for LC-MS/MS analysis.

Lipid analysis with UPLC-ESI-MS/MS

Lipid molecular species were identified using an UPLC (SCIEX ExionLC™ AD, Framingham, USA) and an MS/MS (SCIEX QTRAP® 6500+, Framingham, USA) system (Metware Biotechnology Co., Ltd, http://www.metware.cn/, Wuhan, Hubei, China). A Thermo Accucore™ C30 chromatographic column (2.6 µm, 2.1 mm × 100 mm i.d., Waltham, USA) was used in the LC-ESI-MS/MS system. The mobile phase comprised two components including the A phase that consisted of acetonitrile/water (60/40, v/v) with 0.1% formic acid and 10 mmol/L ammonium formate; and the B phase that constituted acetonitrile/isopropanol (10/90, v/v) with 0.1% formic acid and 10 mmol/L ammonium formate. The gradient elution programs and ESI-MS/MS conditions were set as previously described [45]. A mobile phase flow rate of 0.35 mL/min, a column temperature of 45 °C, and an injection volume of 2 µL were used for each sample.

Identification and quantification of lipid species

The identification of lipid molecular species was based on the in-house MetWare Database (MWDB) that considers the retention times of analytes and parent-daughter ion pair information to enable qualitative analysis [46]. Following methods described in Sect. 2.5, PCA and PLS-DA analyses were used with the lipid profile information. Significantly differentially abundant lipids among groups were identified based on VIP values (VIP ≥ 1) and absolute log2 fold change values ($|\log_2 FC| \geq 1.0$).

Results

Widely targeted metabolome and lipidome profiling of Kentucky bluegrass under cd stress

Pearson correlation analysis among samples revealed that the three biological replicates within each treatment group exhibited correlation coefficients > 0.95, indicating a high level of consistency among samples within treatment groups (Fig. 1A). Further, the PCA of widely targeted metabolome profiles revealed that biological replicates from different treatment groups clustered together, further supporting the high consistency among replicates within treatment groups (Fig. 1B). Additionally, the three QC samples were highly similar and clustered together, confirming the stability of the instrument during measurements and a high level of reliability for the obtained data (Fig. 1B). Flavonoids were the most prevalent metabolites, comprising 15.69% of all metabolites, with phenolic acids (13.47%), alkaloids (11.59%), and amino acids and derivatives (11.54%) following (Fig. 1C). After Cd stress, the M variety exhibited up-regulation of 436 DEMs and down-regulation of 272 DEMs, while the R variety exhibited up-regulation of 450 DEMs and down-regulation of 233 DEMs (Fig. 1D). PCA of the lipidome profiles indicated that samples from the same treatment group clustered together, suggesting high biological replicate consistency for treatments and overall appropriateness for subsequent analyses (Fig. S1). In addition, the QC samples clustered together, suggesting stable measurement conditions and high data quality (Fig. S1). TG were the most abundant lipids detected among all samples, with levels exceeding 40% in each treatment (Fig. 2E–H). After Cd stress, the proportion of LDGTS decreased to the greatest extent in the M and R varieties when compared against the CK treatment (Fig. 2E–H). However, the proportions of most lipid subclasses exhibited only minor changes under Cd stress (Fig. 2E–H). A total of 224 lipid species in the M variety exhibited

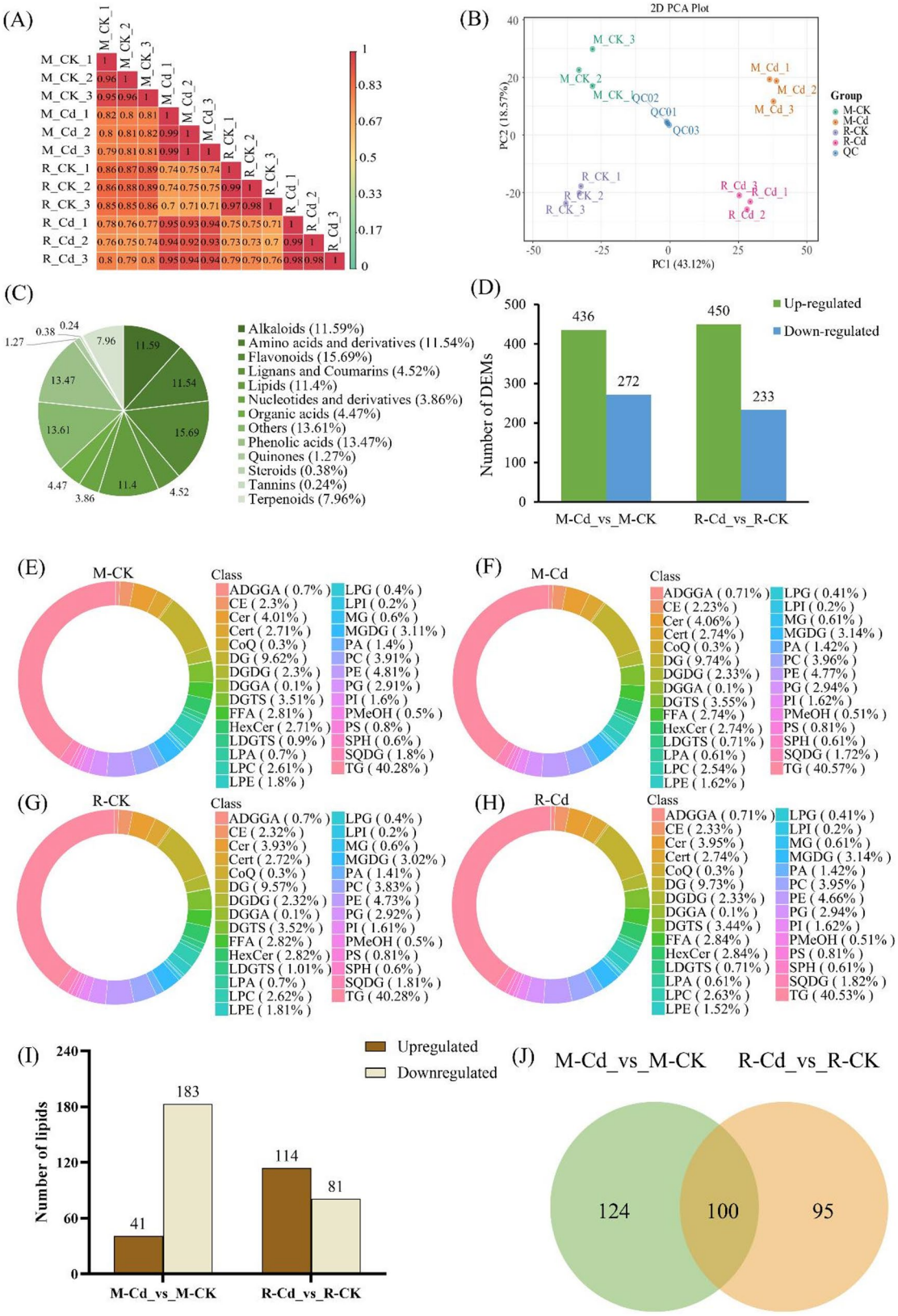

Fig. 1 (See legend on next page.)

(See figure on previous page.)

Fig. 1 Quality assessment of Kentucky bluegrass metabolomes and lipidomes under Cd stress, in addition to classification and differential expression analysis of metabolites. (**A**) Pearson's correlation coefficients among samples. The numbers inside the squares are the correlation coefficients between samples, with deeper red colors indicating stronger positive correlations. (**B**) PCA analysis of metabolites. PC1 is the first principal component, PC2 is the second principal component, and the percentage indicates the explanatory power of each component for the overall dataset. Each point in the figure represents a sample profile, and samples from the same treatment group are shown in the same color. (**C**) Overall metabolite compositions. Each color represents a category of metabolites, with the size of the colored block indicating the proportion of that category. (**D**) Differentially expressed metabolites within the M and R varieties under Cd stress. (**E-H**) Proportion of lipid species in samples from different treatment groups. Each color represents a lipid subclass, with the area of the colored block indicating the proportion of that subclass among the overall profile. (**I**) Differential expression analyses of lipid species under Cd stress. (**J**) Numbers of common and unique differentially expressed lipids in the M and R varieties of Kentucky bluegrass under Cd stress. CK: control group; Cd: treatment group (600 μM of Cd stress); M: Cd-tolerant Kentucky bluegrass variety; R: Cd-sensitive Kentucky bluegrass variety; QC: quality control samples. M-Cd_vs_M-CK and R-Cd_vs_R-CK indicate comparisons of the Cd and CK treatments with the M and R varieties

differential expression under Cd stress, with 41 being up-regulated and 183 being down-regulated (Fig. 2I). However, 114 lipid species were up-regulated in the R variety, while only 81 lipid species were down-regulated (Fig. 2I). Furthermore, among the differentially expressed lipids, a total of 100 were differentially expressed when comparing Cd treatment of both the M and R varieties (Fig. 2J). After Cd stress, 124 lipid species exhibited specific differential abundances in the M variety, while 95 lipid species exhibited specific differential abundances in the R variety (Fig. 2J). These results indicate that under Cd stress, the M and R varieties exhibit markedly different lipid metabolism profiles.

KEGG enrichment and classification of Cd-induced DEMs in the M and R varieties

DEMs in the M variety after Cd stress primarily included those involved in metabolic pathways and the biosynthesis of secondary metabolites (Fig. S2A). In addition, Cd stress-mediated DEMs within the R variety were primarily enriched and in association with pathways of biosynthesis of cofactors and amino acids (Fig. S2A). During Cd stress, pathways including metabolism of nicotinate/nicotinamide, stilbenoid, diarylheptanoid, linoleic acid, arachidonic acid, and sulfur were enriched in both varieties, alongside pathways related to the biosynthesis of amino acids, flavonoids, gingerol, and phenylpropanoid biosynthesis, suggesting a common response to Cd toxicity between the varieties (Fig. S2A). In addition, Cd stress treatment of the M variety led to a greater number of DEMs enriched in pathways including the metabolism of phenylalanine, ascorbate, aldarate, and C5-branched dibasic acid metabolism, in addition to ABC transporters (Fig. S2A). Thus, metabolites in these pathways may play critical roles in Cd tolerance within the M variety. Classification of the Cd stress-mediated DEMs revealed that the highest abundances of phenolic acids and amino acids, in addition to derivatives, were present in both the M and R varieties (Fig. S2B). However, after Cd stress, the abundances of differentially abundant phenolic acids were higher in the R variety than in the M variety, while the abundances of amino acids and derivatives were higher in the M variety than in the R variety (Fig. S2B). It is worth noting that the abundances of differentially abundant terpenoids, including sesquiterpenoids, triterpenes, terpenes, and monoterpenoids, were much higher in the M variety than in the R variety (Fig. S2B).

Pearson correlation analysis reveals key metabolites responsive to cd stress in the M variety

Pearson correlation network analysis revealed a total of 179,509 interactions, with correlation coefficients > 0.9 (Fig. 3A). The 20 most enriched downstream metabolites were further scrutinized, with 10 of these being amino acids or derivatives (Fig. 3B). Additionally, the abundances of saccharides, flavonols, lignans, and alcohols exhibited high correlations with numerous other metabolites (Fig. 3B). Classification of the metabolites within the correlation network revealed that phenolic acids and amino acids (and their derivatives) were the most abundant, followed by flavones, sesquiterpenoids, and alkaloids (Fig. 3C). Moreover, a significant number of lipids, including 21 free fatty acids, 19 lysophosphatidylethanolamines (LPEs), and 15 lysophophatidylcholine (LPCs), were identified (Fig. 3C). Thus, these metabolites may play critical roles in the responses of the Kentucky bluegrass M variety to Cd stress.

Effects of Cd stress on the concentrations of amino acids, phenolic acids, and saccharides in Kentucky bluegrass

Given the critical role of amino acids and derivatives in Cd stress responses, a comparative analysis was conducted of their abundances in the M and R variety roots (Fig. 2, S3A). Both the M and R varieties exhibited increased levels of amino acids and derivatives after Cd stress. Notably, the M variety exhibited more pronounced increases of these compounds relative to the R variety (Fig. 2, S3A). Furthermore, both the M and R varieties exhibited increased saccharide concentrations after Cd stress, with the M variety demonstrating higher saccharide concentrations relative to the R variety after Cd stress (Fig. 2, S3B). The higher concentrations of amino acids, saccharides, and associated derivatives in the M variety likely enhances their tolerance to Cd stress. Considering phenolic acids, a total of 170 differentially abundant phenolic acids were identified in both the M and

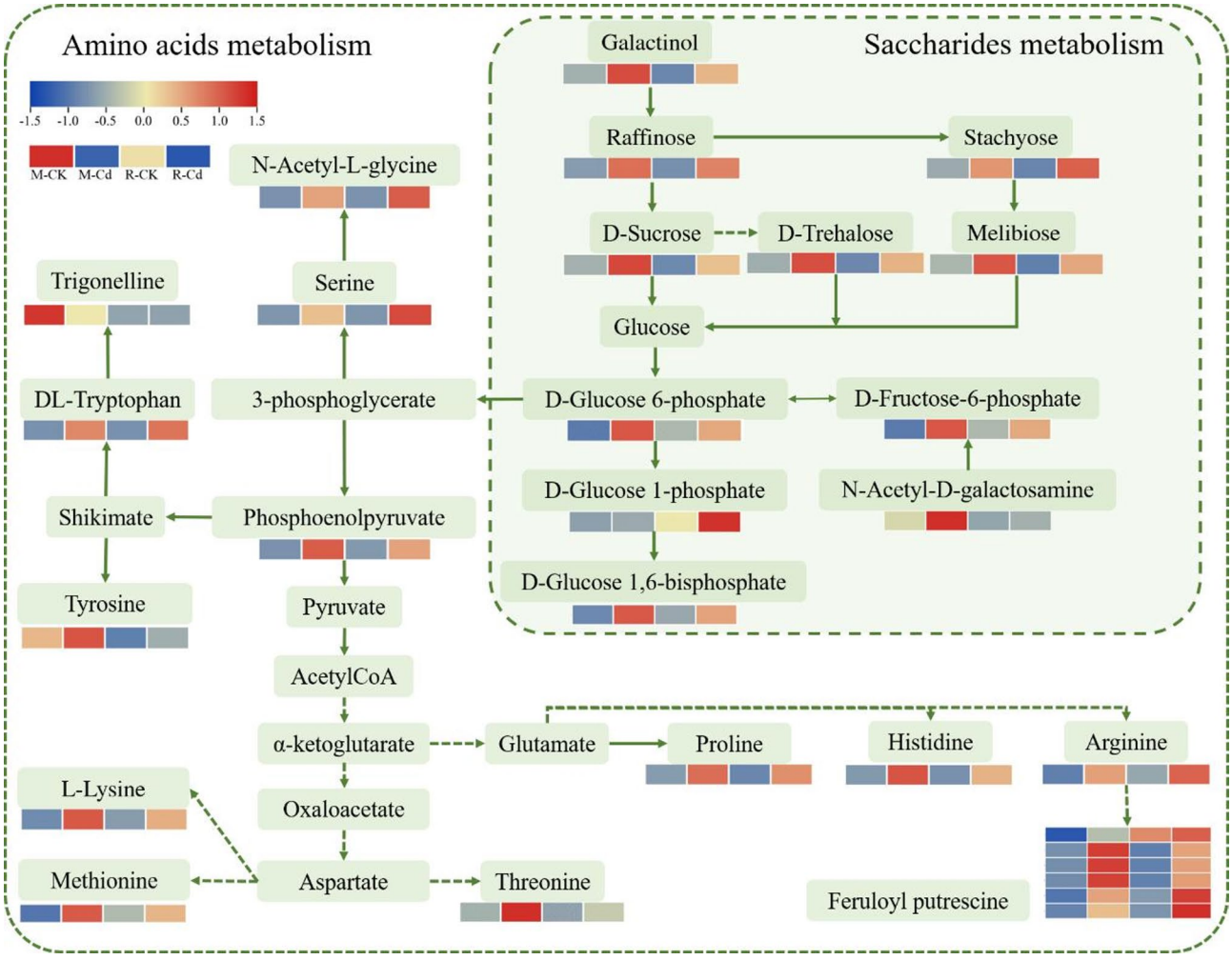

Fig. 2 Abundances of amino acids and saccharides in M and R varieties after Cd stress. Row-scale normalization was applied to the metabolite abundance values prior to heatmap generation. Red colors indicate increased metabolite abundances, while blue colors indicate decreased metabolite abundances. CK: control group; Cd: treatment group (600 μM of Cd stress); M: Cd-tolerant Kentucky bluegrass variety; R: Cd-sensitive Kentucky bluegrass variety

R varieties after Cd stress, with the majority exhibiting increased abundances (Fig. S4). Specifically, 118 phenolic acids were up-regulated in the M variety, while 108 phenolic acids were up-regulated in the R variety (Fig. S4). The observed increases in phenolic acid levels consequently might positively influence the response of Kentucky bluegrass to Cd stress (Fig. S4).

Effects of cd stress on lipid species in Kentucky bluegrass

Both the M and R varieties exhibited decreased total lipid content after Cd stress (Fig. 4A). Further, both varieties exhibited significant increases in acyl diacylglyceryl glucuronide (ADGGA) and monogalactosyldiacylglycerol (MGDG) concentrations after Cd stress (Fig. 4B, Q). Furthermore, both varieties exhibited significant decreases in ceramide (Cer), lysodiacylglyceryl trimethylhomoserine (LDGTS), LPA, and phosphatidic acid (PA) concentrations after Cd stress (Fig. 4D, K, L, R). After Cd stress, the R variety exhibited significantly higher levels of cholesteryl ester (CE), diacylglyceryl glucuronide (DGGA), diacylglyceryl trimethylhomoserine (DGTS), and monogalactosyldiacylglycerol (MGDG) compared to the M variety (Fig. 4C, H, I, Q). In addition, the abundances of Cert, PMeOH, and TG in the M variety were significantly higher than in the R variety after Cd stress (Fig. 4E, S, W).

Although most lipid species in the M and R varieties did not exhibit significantly different abundances when comparing Cd stress and control conditions, noticeable changes were observed in the lengths of the acyl chains of these lipid molecular species (Fig. 5). A significant decrease in free fatty acid (FFA) concentrations were observed in both the M and R varieties after Cd stress (Fig. 5). Further, the concentrations of phosphatidic acid (PA) and lysophosphatidic acid (LPA) with shorter acyl chains were lower in both varieties after Cd stress, while the abundances of diacylglycerol (DG), monogalactosyldiacylglycerol (MGDG), phosphatidylcholine (PC),

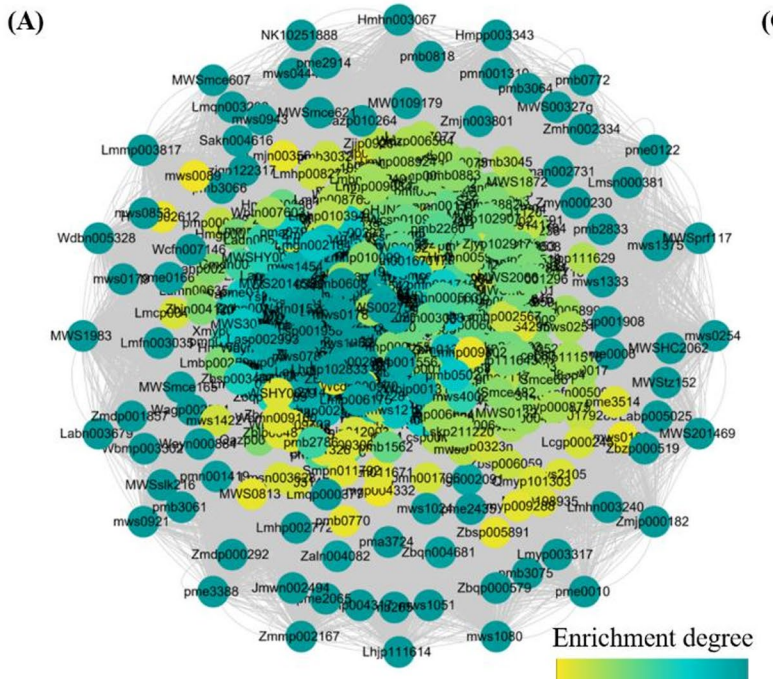

(B) Top 20 enriched metabolites

Metabolic ID	Class	Compounds
mws0254	Amino acids and derivatives	L-Histidine
Wdbn005328	Lignans	3,3'-Bis(3,4-dihydro-4-hydroxy-6,8-dimethoxy-2H-1-benzopyran)
mws0921	Alcohol compounds	p-Coumaryl alcohol
MWS201469	Amino acids and derivatives	Glu-Arg
pmb0772	Plumerane	N-Cinnamoylserotonin
MWSprf117	Amino acids and derivatives	5-Hydroxy-DL-tryptophan(5-HTP)
NK10251888	Amino acids and derivatives	NG,NG-Dimethyl-L-arginine*
Lmmp003817	Flavonols	Kaempferol-3-O-(6"-malonyl) glucoside*
Labn003679	Alcohol compounds	Caffeyl alcohol 4-O-β-D-glucopyranoside
Lhjp111614	Monoterpenoids	Methylasperuloside
pme0010	Amino acids and derivatives	L-Serine
mws1080	Saccharides	Galactinol
MWSmce607	Amino acids and derivatives	DL-Threonine
pme3388	Amino acids and derivatives	Homoarginine
Hmhn003067	Phenolic acids	Phenylpropionic acid-O-β-D-glucopyranoside
MWS1983	Saccharides	Maltitol
Hmpp003343	Ketone compounds	1,7-Bis(4-Hydroxy-3-Methoxyphenyl) Hepta-4,6-Dien-3-One
Zmmp002167	Amino acids and derivatives	L-Glutamyl-L-Tyrosine
pme0122	Amino acids and derivatives	N6-Acetyl-L-lysine
Zmjp000182	Amino acids and derivatives	N-Monomethyl-L-arginine*

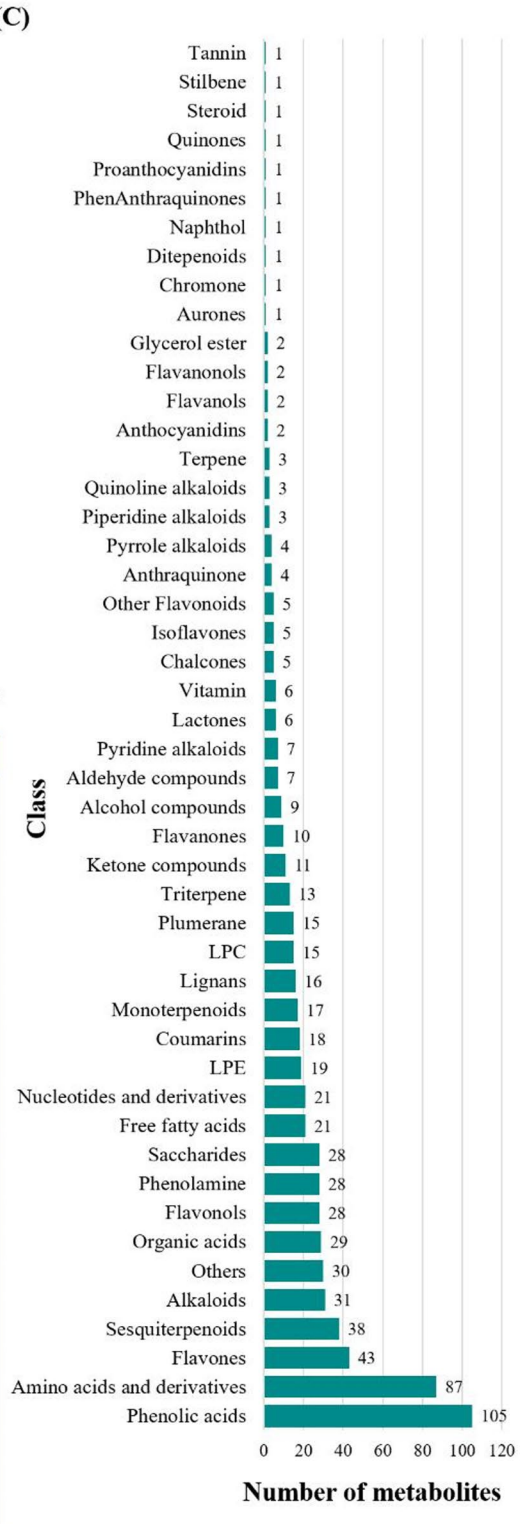

Fig. 3 Hub metabolites involved in the Cd stress response of the Cd-tolerant Kentucky bluegrass variety M. (**A**) Pearson correlation network of DEM abundances within the Cd-tolerant varieties M. The relationships in the network represent Pearson coefficients (those that were > 0.9), where darker shades of green indicate higher enrichment. (**B**) The 20 most enriched metabolites after Cd stress in the Cd-tolerant variety M. (**C**) Classification of metabolites within the correlation network

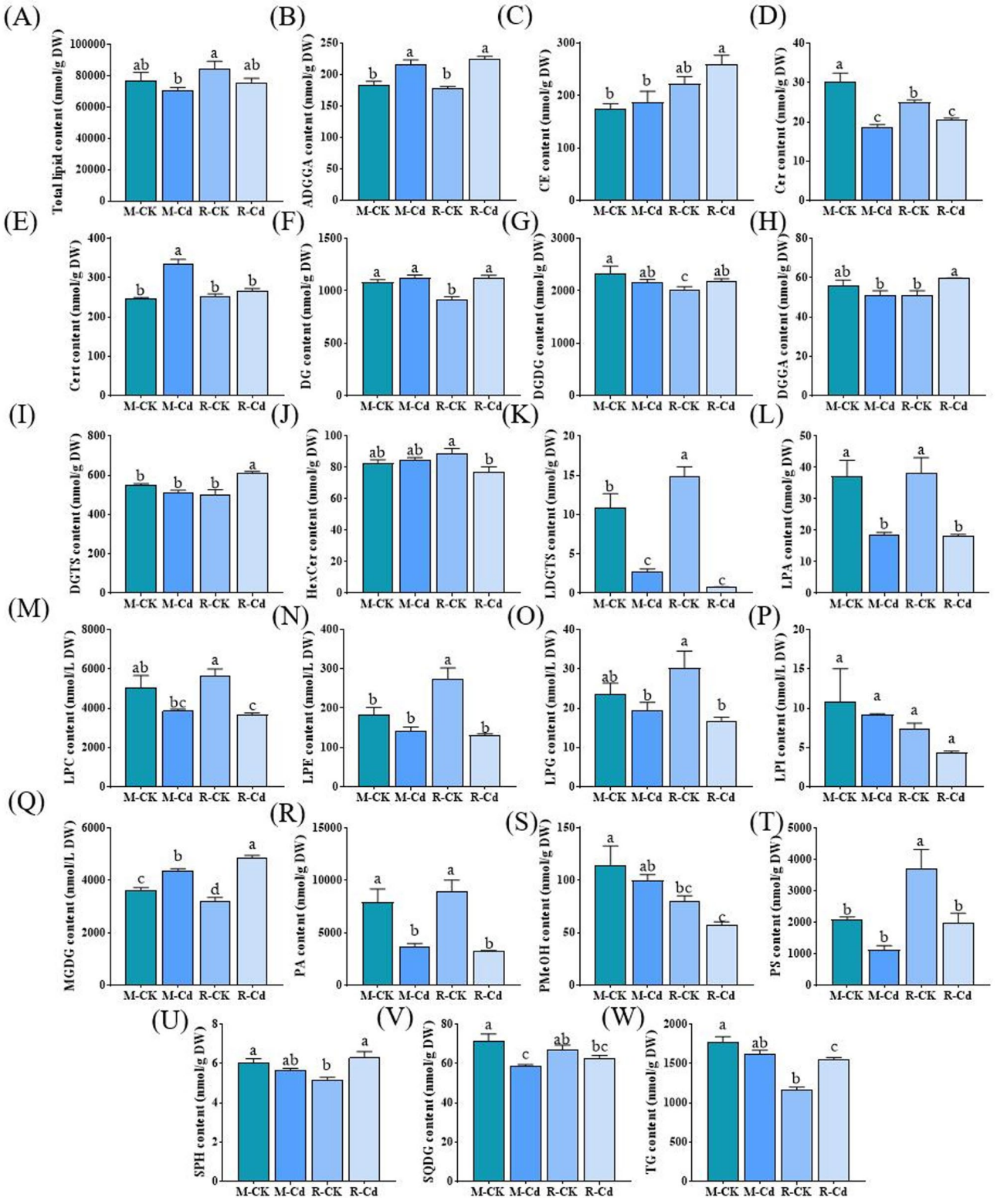

Fig. 4 Effects of Cd stress on the abundances of total lipids and different lipid species in Kentucky bluegrass. Data are expressed as means ± SE ($n = 3$), with different letters indicate significant differences ($p < 0.05$, one-way ANOVA). ADGGA: Acyl diacylglyceryl glucuronide; CE: Cholesteryl ester; Cer: Ceramide; Cert: Phytoceramide; DG: Diacylglycerol; DGDG: Digalactosyldiacylglycerol; DGGA: Diacylglyceryl glucuronide; DGTS: Diacylglyceryl trimethylhomoserine; HexCer: Hexosylceramide; LDGTS: Lysodiacylglyceryl trimethylhomoserine; LPA: Lysophosphatidic acid; LPC: Lysophophatidylcholine; LPE: Lysophosphatidylethanolamine; LPG: Lysophosphatidylglycerol; LPI: Lysophosphatidylinositol; MGDG: Monogalactosyldiacylglycerol; PA: Phosphatidic acid; PMeOH: Phosphatidylmethanol; PS: Phosphatidylserine; SPH: sphingosine; SQDG: Sulfoquinovosyl diacylglycerol; TG: Triacylglycerol. CK: control group; Cd: treatment group (600 μM of Cd stress); M: Cd-tolerant Kentucky bluegrass variety; R: Cd-sensitive Kentucky bluegrass variety

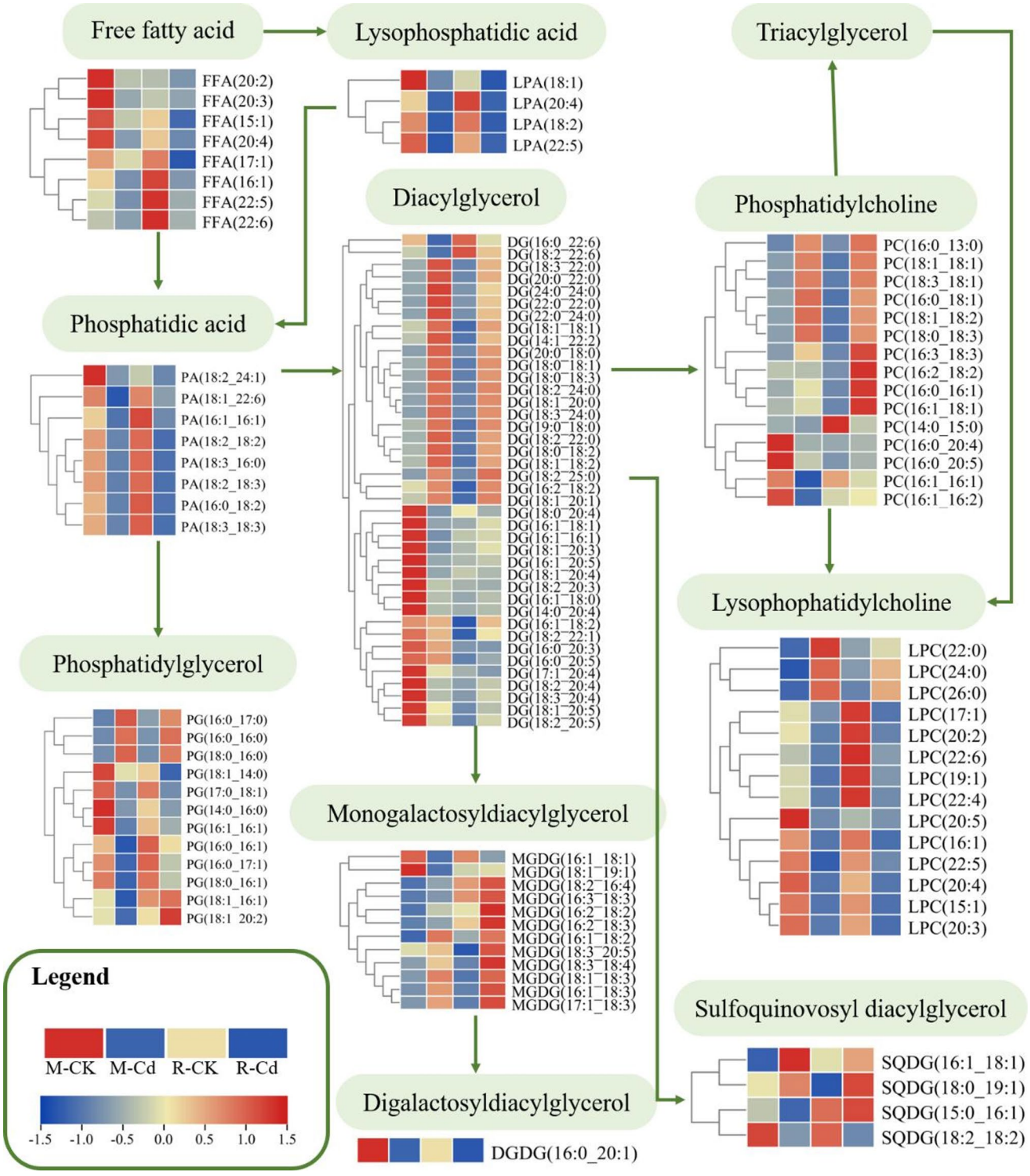

Fig. 5 Abundances of lipid species in the Kentucky bluegrass M and R varieties after Cd stress. Row-scale normalization was applied to metabolite values prior to heatmap construction. Red colors indicate increased concentrations of metabolite abundance, while blue colors indicate decreased metabolite abundances. CK: control group; Cd: treatment group (600 μM of Cd stress); M: Cd-tolerant Kentucky bluegrass variety; R: Cd-sensitive Kentucky bluegrass variety. Different lipid species are shown based on different acyl chains: double bonds

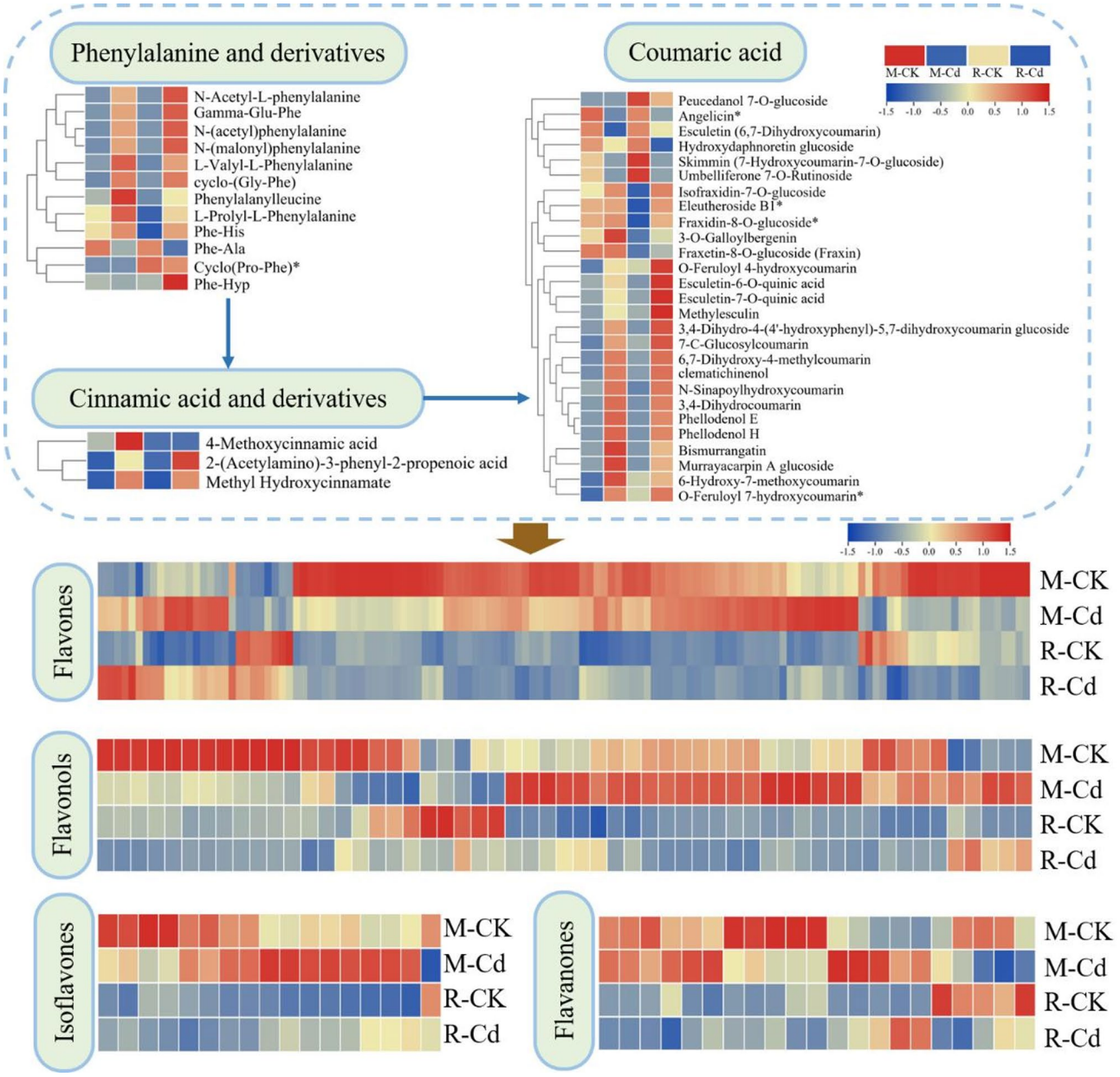

Fig. 6 Abundances of flavonoids in M and R varieties after Cd stress. Row-scale normalization was applied to metabolite values prior to heatmap construction. Red colors indicate increased concentrations of metabolite abundance, while blue colors indicate decreased metabolite abundances. CK: control group; Cd: treatment group (600 μM of Cd stress); M: Cd-tolerant Kentucky bluegrass variety; R: Cd-sensitive Kentucky bluegrass variety. Different lipid species are shown based on different acyl chains: double bonds

triacylglycerol (TG), and lysophosphatidylcholine (LPC) with longer acyl chains increased in both varieties after Cd stress (Fig. 5, S5). Thus, the elongation of lipid acyl chains may represent an important response of Kentucky bluegrass to Cd stress.

Effects of cd stress on flavonoid concentrations in Kentucky bluegrass

After Cd stress, the abundances of phenylalanine, coumaric acid, cinnamic acid, and their derivatives increased in the M and R varieties (Fig. 6). These metabolites serve as precursors in the synthesis of flavones, flavonols, isoflavones, and flavanones (Fig. 6). Under both Cd stress and control conditions, the M variety exhibited higher abundances of flavones, flavonols, isoflavones, and flavanones compared to the R variety, which may be related to responses to Cd stress (Fig. 6).

Discussion

Lipid remodeling is involved in the cd stress responses of Kentucky bluegrass

VLCFAs are considered key substrates in suberin biosynthesis [23, 47]. Moreover, VLCFAs play important roles as essential precursors in the biosynthesis of triacylglycerols, waxes, phospholipids, and complex sphingolipids [48]. Abiotic stresses including salinity, low temperatures, and exposure to heavy metals may elevate levels of VLCFAs in different plant species [49]. Nevertheless, several studies have demonstrated that exposure to Cd leads to markedly lower levels of VLCFAs in *Triticum aestivum* [50], *Catharanthus roseus* [51], and *Linum usitatissimum* [52]. The concentrations of VLCFAs in Kentucky bluegrass varieties M and R decreased in response to Cd stress in the short-term (Fig. 5). However, Cd stress led to increased Cert, DG, MGDG PC, and TG levels in both M and R varieties (Figs. 4 and 5 and S5). The synthesis of these lipid species may result in depletion of FAA and PA [53]. Moreover, increased levels of saturated PG, DG, TG, PC, and LPC lipid species were observed in both M and R varieties under Cd stress accompanied by decreased levels of unsaturated PG, DG, TG, PC, and LPC lipid species that have an increased numbers of double bonds (Fig. 5, S5). Lipids with long and saturated fatty acids increase membrane thickness and rigidity due to dense packing of hydrophobic tails and enhanced lipid-lipid interactions [54]. Consequently, the elongation of acyl chains and reduced number of unsaturated double bonds in lipids of the M and R varieties under Cd stress could be key mechanisms involved in their adaptation to the stress. Comparable regulatory patterns were also observed in the roots of *Triticum aestivum* that were subjected to Cd stress [55].

The ratios of DGDG/MGDG and PC/PE are critical indicators that can enable assessment of plasma membrane stability [31]. A recent study [55] demonstrated a positive correlation between DGDG/MGDG and PC/PE ratios with plasma membrane stability. After Cd stress, the DGDG/MGDG and PC/PE ratios of the M variety exceeded those of the R variety (Fig. S6), indicating greater plasma membrane stability within the M variety. Another study [56] also revealed that the drought and salt-tolerant *Gossypium* cultivar exhibited elevated DGDG/MGDG ratios. Moreover, wheat has been shown to exhibit an increased PC/PE ratio under heat stress [57].

Increased saccharide and amino acid concentrations contribute to enhanced cd tolerance in Kentucky bluegrass

Cell wall polysaccharides exhibit abundant hydroxyl and carboxyl groups, offering abundant binding sites for Cd ion complexing [58]. D-fructose-6-phosphate and D-glucose-6-phosphate are key metabolites in the galactose metabolism pathway and are essential precursors of cell wall polysaccharides [6, 25]. Further, the overexpression of *raffinose synthase* has been shown to increase drought tolerance of *Zea mays* and *Arabidopsis thaliana* by stimulating raffinose synthesis [59]. The M variety exhibited increased levels of metabolites related to galactose metabolism including galactinol, raffinose, stachyose, D-sucrose, D-fructose-6-phosphate, D-glucose-6-phosphate, N-acetyl-D-galactosamine, and melibiose after Cd stress, potentially enhancing its tolerance to Cd-induced stress through the biosynthesis of cell wall polysaccharides. We previously showed that the M variety of Kentucky bluegrass exhibits a higher concentration of hemicellulose in root cell walls compared to the R variety, consistent with this observation [6]. *Fagopyrum tataricum* [60], *Triticum aestivum* [61], and *Medicago sativa* [62] also exhibit enrichment of genes and metabolites associated with galactose metabolism after Cd stress.

The majority of amino acids exhibit abundances with significant positive correlations to Cd accumulation and resistance in plants [63–65]. Cd stress can induce the synthesis of heavy metal-associated transporters in plants [66]. The metal-binding domains of heavy metal-associated transporters in plants contain significant proportions of cysteine, aspartic acid, glutamic acid, histidine, and methionine amino acid residues [67]. The elevated levels of S-(5'-adenosy)-L-homocysteine, N-alpha-acetyl-L-asparagine, L-aspartic acid-O-diglucoside, L-homoglutamic acid, L-histidine, S-(5'-adenosyl)-L-methionine, L-homomethionine, and S-adenosylmethionine in both the M and R varieties could potentially enhance Cd accumulation and tolerance in Kentucky bluegrass (Fig. 2, S3A). Moreover, the M variety exhibited elevated levels of various free amino acids (DL-threonine, L-saccharopine, L-threonine, L-homoserine, 3-(pyrazol-1-yl)-L-alanine, L-γ-glutamyl-L-leucine, N-γ-acetyl-L-ornithine, L-histidine, L-glutamyl-L-tyrosine, L-valyl-L-phenylalanine, L-lysine, N-malonylleucine, and N-acetyl-tryptophan) after Cd stress, potentially improving its Cd tolerance (Fig. 2, S3A). Similarly, higher levels of free amino acids were detected in the Cd-tolerant plant *Crassocephalum crepidioides* relative to the Cd-sensitive plant *Ageratum conyzoides* [68].

Nitric oxide and polyamines play important roles as signaling molecules in plant responses to environmental stress [24, 69]. Further, arginine is a precursor for both polyamines and nitric oxide [70]. Increased expression of the superoxide dismutase gene SOD1 in *Arabidopsis* enhances spermidine accumulation, thereby improving tolerance to Cd [71]. Under Cd stress, the M variety of Kentucky bluegrass demonstrated increased levels of arginine and its derivatives, including homoarginine, arginine methyl ester, N-monomethyl-L-arginine, NG, NG-dimethyl-L-arginine, and N, N'-dimethylarginine,

suggesting an important function of enhanced arginine metabolism in mitigating Cd-induced stress (Fig. 2, S3A). Increased arginine levels induced by Cd stress have also been reported in *Oryza sativa* [9].

Enhanced tolerance to cd in the M variety via increased flavonoid levels

Flavonoids exhibit cytoprotective effects against Cd-induced diseases by scavenging reactive oxygen species, chelating Cd to reduce its biotoxicity, and mitigating DNA damage while inhibiting apoptosis [72]. Phenylalanine metabolism is the essential pathway for synthesizing flavonoids [73]. In addition, Coumaric and cinnamic acids are crucial metabolites within phenylpropane metabolism [74]. Accordingly, the increased abundances of phenylalanine, coumaric acid, cinnamic acid, flavonoids, and their derivatives in the M and R varieties under Cd stress indicates the involvement of phenylpropane metabolism-mediated flavonoid biosynthesis in responding to Cd stress (Fig. 6, Table S1). Consistently, phenylpropane metabolism contributes to the responses of *Cucumis melo* [75], *Tagetes patula* [76], and *Oryza sativa* [77] to Cd stress. The elevated levels of flavonoids in the M variety relative to the R variety in both the control and Cd treatment conditions could significantly contribute to the observed enhanced tolerance to Cd-induced stress (Fig. 6, Table S1). Consistently, the drought-tolerant *Triticum aestivum* demonstrated elevated expression of genes involved in flavonoid biosynthesis and higher flavonoid content in contrast to the sensitive variety [78].

Conclusions

The global metabolomic and lipidomic analyses of this study revealed a comprehensive metabolic landscape of Kentucky bluegrass in response to Cd stress. Cd stress triggered lipid restructuring in both the M and R varieties of Kentucky bluegrass, leading to increased lengths of acyl chains in lipid species and saturation levels of PG, DG, TG, PC, and LPC. Further, the elevated concentrations of amino acids (DL-threonine, L-saccharopine, L-threonine, L-homoserine, 3-(pyrazol-1-yl)-L-alanine, L-γ-glutamyl-L-leucine, N-γ-acetyl-L-ornithine, L-histidine, L-glutamyl-L-tyrosine, L-valyl-L-phenylalanine, L-lysine, N-malonylleucine, and N-acetyl-tryptophan), saccharides (galactinol, raffinose, stachyose, D-sucrose, D-fructose-6-phosphate, D-glucose-6-phosphate, N-acetyl-D-galactosamine, and melibiose), flavonoids (flavones, flavonols, isoflavones, and flavanones), and their derivatives in the M variety (but not the R variety) under Cd stress may enable enhanced tolerance to Cd. However, the roles of these key metabolites in Cd detoxification and transport require further validation. In subsequent studies, these key metabolites may be exogenously applied or genetically modulated in planta to coordinate cadmium detoxification or accumulation dynamics.

Abbreviations

Cd	Cadmium
M	Midnight
R	Rugby II
QC	Quality control
PCA	Principal component analysis
PLS-DA	Partial Least Squares-Discriminant Analysis
OSC	Orthogonal signal correction
DEMs	Differentially expressed metabolites
VIP	Variable importance in projection
FC	Fold-change
KEGG	Kyoto Encyclopedia of Genes and Genomes
MWDB	MetWare Database
LPEs	Lysophosphatidylethanolamines
LPCs	Lysophophatidylcholine
ADGGA	Acyl diacylglyceryl glucuronide
MGDG	Monogalactosyldiacylglycerol
Cer	Ceramide
LDGTS	Lysodiacylglyceryl trimethylhomoserine
PA	Phosphatidic acid
CE	Cholesteryl ester
DGGA	Diacylglyceryl glucuronide
DGTS	Diacylglyceryl trimethylhomoserine
MGDG	Monogalactosyldiacylglycerol
Cert	Phytoceramide
Cert	Phytoceramide
DG	Diacylglycerol
DGDG	Digalactosyldiacylglycerol
DGTS	Diacylglyceryl trimethylhomoserine
HexCer	Hexosylceramide
LDGTS	Lysodiacylglyceryl trimethylhomoserine
LPA	Lysophosphatidic acid
LPC	Lysophophatidylcholine
LPE	Lysophosphatidylethanolamine
LPG	Lysophosphatidylglycerol
LPI	Lysophosphatidylinositol
MGDG	Monogalactosyldiacylglycerol
PMeOH	Phosphatidylmethanol
PS	Phosphatidylserine
SPH	Sphingosine
SQDG	Sulfoquinovosyl diacylglycerol
TG	Triacylglycerol
FFA	Fatty acid
PC	Phosphatidylcholine
TG	Triacylglycerol

Supplementary Information

The online version contains supplementary material available at https://doi.org/10.1186/s12870-025-06709-1.

Supplementary Material 1: Table S1. Cd-induced flavonoids in the roots of M and R varieties.

Supplementary Material 2: Fig. S1 PCA of lipids content in different samples.

Supplementary Material 3: Fig. S2 KEGG enrichment analysis (A) and classification (B) of DEMs in the M and R varieties under Cd stress.

Supplementary Material 4: Fig. S3 Effects of Cd stress on the amino acids and derivatives (A), and saccharides (B) content in the Cd-tolerant variety M and Cd-sensitive variety R.

Supplementary Material 5: Fig. S4 Effects of Cd stress on the phenolic acids content in the Cd-tolerant variety M and Cd-sensitive variety R.

Supplementary Material 6: Fig. S5 Effects of Cd stress on the triacylglycerol (TG) content in the Cd-tolerant variety M and Cd-sensitive variety R.

Supplementary Material 7: Fig. S6 Ratios of DGDG/MGDG (A) and PC/PE (B) of M and R varieties under Cd stress.

Acknowledgements
We thank LetPub (www.letpub.com.cn) for linguistic assistance and pre-submission expert review.

Author contributions
HLM and TC conceived and designed the experiment. TC, YW and CXZ performed the experiments. TC, YW and KJN analyzed all the data. TC wrote the manuscript. HLM revised the manuscript. All authors contributed to the acquisition of data, interpretation of results and critical discussion and approved the final version of the manuscript.

Funding
This work was supported by the Open Competition Projects to Select the Best Candidates for Leading Key Initiatives of the Key Laboratory of Grassland Ecosystems, Gansu Agricultural University, Ministry of Education [grant number KLGE-2024-03], the National Natural Science Foundation of China [grant number 32071886], the Youth PhD Funding Project From Gansu Provincial Education Department [grant number 2024QB-075], and the Fostering Foundation for the Excellent Ph. D. Dissertation of Gansu Agricultural University [grant number YB2022003].

Data availability
All of the datasets supporting the results of this article are included within the article and its Additional files. Metabolome data that support the fingdings of this study have been deposited in the MetaboLights, with the primary accession code REQ20250402209743.

Declarations

Ethics approval and consent to participate
This article does not contain any studies with animals or humans performed by any of the authors. This study complies with institutional, national and international guidelines and legislation.

Consent for publication
Not applicable.

Competing interests
The authors declare no competing interests.

Author details
[1]Key Laboratory of Grassland Ecosystem (Gansu Agricultural University), Ministry of Education, College of Pratacultural Science, Ministry of Education Pratacultural Engineering Laboratory of Gansu Province, Gansu Agricultural University, Sino-U.S. Center for Grazingland Ecosystem Sustainability, Yingmencun, Anning District, Lanzhou, Gansu 730070, China

Received: 2 April 2025 / Accepted: 13 May 2025
Published online: 20 May 2025

References

1. Huang W, Sun D, Zhao T, Long K, Zhang Z. Spatial–temporal distribution and source analysis of atmospheric particulate-bound cadmium from 1998 to 2021 in China. Environ Geochem Health. 2024;46:44.
2. Liu H, Wang H, Zhou J, Zhang Y, Wang H, Li M, Wang X. Environmental cadmium pollution and health risk assessment in rice–wheat rotation area around a smelter. Environ Sci Pollut Res. 2024;31:433–44.
3. Jiang Z, Guo Z, Peng C, Liu X, Zhou Z, Xiao X. Heavy metals in soils around non-ferrous smelteries in China: status, health risks and control measures. Environ Pollut. 2021;282:117038.
4. Shi J-J, Shi Y, Feng Y-L, Li Q, Chen W-Q, Zhang W-J, Li H-Q. Anthropogenic cadmium cycles and emissions in Mainland China 1990–2015. J Clean Prod. 2019;230:1256–65.
5. Shen C, Huang B, Hu L, Yuan H, Huang Y, Wang Y, Sun Y, Li Y, Zhang J, Xin J. Comparative transcriptome analysis and *Arabidopsis thaliana* overexpression reveal key genes associated with cadmium transport and distribution in root of two *Capsicum annuum* cultivars. J Hazard Mater. 2024;465:133365.
6. Wang Y, Cui T, Niu K, Ma H. Integrated proteomics, transcriptomics, and metabolomics offer novel insights into cd resistance and accumulation in Poa pratensis. J Hazard Mater. 2024. 134727.
7. Zhang Z-H, Zhou T, Tang T-J, Song H-X, Guan C-Y, Huang J-Y, Hua Y-P. A multiomics approach reveals the pivotal role of subcellular reallocation in determining rapeseed resistance to cadmium toxicity. J Exp Bot. 2019;70:5437–55.
8. Niu K, Zhu R, Wang Y, Zhao C, Ma H. 24-epibrassinolide improves cadmium tolerance and lateral root growth associated with regulating endogenous auxin and ethylene in Kentucky bluegrass. Ecotoxicol Environ Saf. 2023;249:114460.
9. Jiang M, Jiang J, Li S, Li M, Tan Y, Song S, Shu Q, Huang J. Glutamate alleviates cadmium toxicity in rice via suppressing cadmium uptake and translocation. J Hazard Mater. 2020;384:121319.
10. Cui T, Wang Y, Niu K, Dong W, Zhang R, Ma H. Auxin alleviates cadmium toxicity by increasing vacuolar compartmentalization and decreasing long-distance translocation of cadmium in Poa pratensis. J Plant Physiol. 2023;282:153919.
11. Niu K, Zhang R, Zhu R, Wang Y, Zhang D, Ma H. Cadmium stress suppresses the tillering of perennial ryegrass and is associated with the transcriptional regulation of genes controlling axillary bud outgrowth. Ecotoxicol Environ Saf. 2021;212:112002.
12. Reeves RD, Baker AJM, Jaffré T, Erskine PD, Echevarria G, van der Ent A. A global database for plants that hyperaccumulate metal and metalloid trace elements. New Phytol. 2018;218:407–11.
13. Niu K, Ma H. The positive effects of exogenous 5-aminolevulinic acid on the chlorophyll biosynthesis, photosystem and Calvin cycle of Kentucky bluegrass seedlings in response to osmotic stress. Environ Exp Bot. 2018;155:260–71.
14. Wang Y, Cui T, Niu K, Ma H. Comparison and characterization of oxidation resistance and carbohydrate content in cd-Tolerant and -Sensitive Kentucky bluegrass under cd stress. Agronomy. 2021;11:2358.
15. Wang S, Dong Q, Wang Z. Differential effects of citric acid on cadmium uptake and accumulation between tall fescue and Kentucky bluegrass. Ecotoxicol Environ Saf. 2017;145:200–6.
16. Xian J, Wang Y, Niu K, Ma H, Ma X. Transcriptional regulation and expression network responding to cadmium stress in a Cd-tolerant perennial grass *Poa Pratensis*. Chemosphere. 2020;250:126158.
17. Xu P, Wang Z. A comparison study in cadmium tolerance and accumulation in two Cool-Season turfgrasses and Solanum nigrum L. Water Air Soil Pollut. 2014;225:1938.
18. Wu X, Tian H, Li L, Guan C, Zhang Z. Higher cd-accumulating oilseed rape has stronger cd tolerance due to stronger cd fixation in pectin and hemicellulose and higher cd chelation. Environ Pollut. 2021;285:117218.
19. Cornu J-Y, Deinlein U, Höreth S, Braun M, Schmidt H, Weber M, Persson D, Husted S, Schjoerring J, Clemens S. Contrasting effects of Nicotianamine synthase knockdown on zinc and nickel tolerance and accumulation in the zinc/cadmium hyperaccumulator Arabidopsis Halleri. New Phytol. 2015;206:738–50.
20. Yu Y, Wang Q, Wan Y, Huang Q, Li H. Transcriptome analysis reveals different mechanisms of selenite and selenate regulation of cadmium translocation in *Brassica rapa*. J Hazard Mater. 2023;452:131218.
21. Li G-Z, Chen S-J, Li N-Y, Wang Y-Y, Kang G-Z. Exogenous glutathione alleviates cadmium toxicity in wheat by influencing the absorption and translocation of cadmium. Bull Environ Contam Toxicol. 2021;107:320–6.
22. Peng J-S, Wang Y-J, Ding G, Ma H-L, Zhang Y-J, Gong J-M. A pivotal role of cell wall in cadmium accumulation in the Crassulaceae hyperaccumulator Sedum Plumbizincicola. Mol Plant. 2017;10:771–4.
23. Tao Q, Li M, Xu Q, Kováč J, Yuan S, Li B, Li Q, Huang R, Gao X, Wang C. Radial transport difference mediated by root endodermal barriers contributes to differential cadmium accumulation between Japonica and indica subspecies of rice (Oryza sativa L). J Hazard Mater. 2022;425:128008.
24. Imran M, Hussain S, Iqbal A, Saleem MH, Rehman N, ur, Mo Z, Chen X, Tang X. Nitric oxide confers cadmium tolerance in fragrant rice by modulating physio-biochemical processes, yield attributes, and grain quality traits. Ecotoxicol Environ Saf. 2023;261:115078.
25. Shi Y-Z, Zhu X-F, Wan J-X, Li G-X, Zheng S-J. Glucose alleviates cadmium toxicity by increasing cadmium fixation in root cell wall and sequestration into vacuole in Arabidopsis. J Integr Plant Biol. 2015;57:830–7.

26. Wang K, Li F, Gao M, Huang Y, Song Z. Mechanisms of trehalose-mediated mitigation of cd toxicity in rice seedlings. J Clean Prod. 2020;267:121982.
27. Ma Y, Jie H, Zhao L, He P, Lv X, Xu Y, Zhang Y, Xing H, Jie Y. *BnXTH1* regulates cadmium tolerance by modulating vacuolar compartmentalization and the cadmium binding capacity of cell walls in Ramie (*Boehmeria nivea*). J Hazard Mater. 2024;470:134172.
28. Wang L, Li R, Yan X, Sun Y, Xu Y. Pivotal role for root cell wall polysaccharides in cultivar-dependent cadmium accumulation in Brassica chinensis L. Ecotoxicol Environ Saf. 2020;194:110369.
29. Yu H, Guo J, Li Q, Zhang X, Huang H, Huang F, Yang A, Li T. Characteristics of cadmium immobilization in the cell wall of root in a cadmium-safe rice line (Oryza sativa L). Chemosphere. 2020;241:125095.
30. Nouairi I, Ammar WB, Youssef NB, Daoud DBM, Ghorbal MH, Zarrouk M. Comparative study of cadmium effects on membrane lipid composition of *Brassica juncea* and *Brassica napus* leaves. Plant Sci. 2006;170:511–9.
31. Zhang X, Xu Y, Huang B. Lipidomic reprogramming associated with drought stress priming-enhanced heat tolerance in tall fescue (Festuca arundinacea). Plant Cell Environ. 2019;42:947–58.
32. Wang R, Li B, Lam SM, Shui G. Integration of lipidomics and metabolomics for in-depth Understanding of cellular mechanism and disease progression. J Genet Genomics. 2020;47:69–83.
33. Li W, Wen L, Chen Z, Zhang Z, Pang X, Deng Z, Liu T, Guo Y. Study on metabolic variation in whole grains of four proso millet varieties reveals metabolites important for antioxidant properties and quality traits. Food Chem. 2021;357:129791.
34. Buffagni V, Zhang L, Senizza B, Rocchetti G, Ferrarini A, Miras-Moreno B, et al. Metabolomics and lipidomics insight into the effect of different polyamines on tomato plants under non-stress and salinity conditions. Plant Sci. 2022;322:111346.
35. Bulut M, Wendenburg R, Bitocchi E, Bellucci E, Kroc M, Gioia T, Susek K, Papa R, Fernie A, Alseekh S. A comprehensive metabolomics and lipidomics atlas for the legumes common bean, Chickpea, lentil and lupin. Plant J. 2023;116:1152–71.
36. Xian J, Chai S, Wang Y, Niu K, Dong W, Ma H, Zhang R. Effect of cadmium stress on growth and physiological metabolism of Kentucky bluegrass. J Nucl Agric Sci. 2019;33:176–86.
37. Hoagland DR. Optimum nutrient solutions for plants. Science. 1920. https://doi.org/10.1126/science.52.1354.562.
38. Ouyang W, Ning J, Zhu X, Jiang Y, Wang J, Yuan H, Hua J. UPLC-ESI-MS/MS analysis revealed the dynamic changes and conversion mechanism of non-volatile metabolites during green tea fixation. LWT. 2024;198:116010.
39. Zhou J, Fang T, Li W, Jiang Z, Zhou T, Zhang L, Yu Y. Widely targeted metabolomics using UPLC-QTRAP-MS/MS reveals chemical changes during the processing of black tea from the cultivar *Camellia sinensis* (L.) O. Kuntze Cv. Huangjinya. Food Res Int. 2022;162:112169.
40. Chen W, Gong L, Guo Z, Wang W, Zhang H, Liu X, Yu S, Xiong L, Luo J. A novel integrated method for Large-Scale detection, identification, and quantification of widely targeted metabolites: application in the study of rice metabolomics. Mol Plant. 2013;6:1769–80.
41. Fraga CG, Clowers BH, Moore RJ, Zink EM. Signature-Discovery approach for sample matching of a Nerve-Agent precursor using liquid Chromatography– Mass spectrometry, XCMS, and chemometrics. Anal Chem. 2010;82:4165–73.
42. Chen Y, Zhang R, Song Y, He J, Sun J, Bai J, An Z, Dong L, Zhan Q, Abliz Z. RRLC-MS/MS-based metabonomics combined with in-depth analysis of metabolic correlation network: finding potential biomarkers for breast cancer. Analyst. 2009;134:2003–11.
43. Thévenot EA, Roux A, Xu Y, Ezan E, Junot C. Analysis of the human adult urinary metabolome variations with age, body mass index, and gender by implementing a comprehensive workflow for univariate and OPLS statistical analyses. J Proteome Res. 2015;14:3322–35.
44. Kanehisa M, Goto S. KEGG: Kyoto encyclopedia of genes and genomes. Nucleic Acids Res. 2000;28:27–30.
45. Li Q, Zhang W, Shen D, Li Z, Shu J, Liu Y. Comprehensive lipidomics analysis reveals the changes in lipid profile of camellia oil affected by insect damage. Front Nutr. 2022;9.
46. Zhong R, Zhu Y, Zhang H, Huo Y, Huang Y, Cheng W, Liang P. Integrated lipidomic and transcriptomic analyses reveal the mechanism of large yellow croaker roe phospholipids on lipid metabolism in normal-diet mice. Food Funct. 2022;13:12852–69.
47. Franke RB, Dombrink I, Schreiber L. Suberin Goes genomics: use of a short living plant to investigate a long lasting polymer. Front Plant Sci. 2012;3.
48. Bach L, Faure J-D. Role of very-long-chain fatty acids in plant development, when chain length does matter. CR Biol. 2010;333:361–70.
49. De Bigault Du Granrut A, Cacas J-L. How Very-Long-Chain fatty acids could signal stressful conditions in plants?? Front Plant Sci. 2016;7.
50. Ghasemzadeh N, Iranbakhsh A, Oraghi-Ardebili Z, Saadatmand S, Jahanbakhsh-Godehkahriz S. Cold plasma can alleviate cadmium stress by optimizing growth and yield of wheat (Triticum aestivum L.) through changes in physio-biochemical properties and fatty acid profile. Environ Sci Pollut Res. 2022;29:35897–907.
51. Rani S, Singh V, Sharma MK, Sisodia R. GC–MS based metabolite profiling of medicinal plant-Catharanthus roseus under cadmium stress. Plant Physiol Rep. 2021;26:491–502.
52. Belkadhi A, De Haro A, Obregon S, Chaïbi W, Djebali W. Positive effects of Salicylic acid pretreatment on the composition of flax plastidial membrane lipids under cadmium stress. Environ Sci Pollut Res. 2015;22:1457–67.
53. Yu L, Zhou C, Fan J, Shanklin J, Xu C. Mechanisms and functions of membrane lipid remodeling in plants. Plant J. 2021;107:37–53.
54. Harayama T, Riezman H. Understanding the diversity of membrane lipid composition. Nat Rev Mol Cell Biol. 2018;19:281–96.
55. Wu S, Hu C, Wang X, Wang Y, Yu M, Xiao H, Shabala S, Wu K, Tan Q, Xu S, Sun X. Cadmium-induced changes in composition and co-metabolism of glycerolipids species in wheat root: glycerolipidomic and transcriptomic approach. J Hazard Mater. 2022;423:127115.
56. Liu B, Wang X, Li K, Cai Z. Spatially resolved metabolomics and lipidomics reveal salinity and Drought-Tolerant mechanisms of cottonseeds. J Agric Food Chem. 2021;69:8028–37.
57. Hu H, Jia Y, Hao Z, Ma G, Xie Y, Wang C, Ma D. Lipidomics-based insights into the physiological mechanism of wheat in response to heat stress. Plant Physiol Biochem. 2023;205:108190.
58. Krzeslowska M. The cell wall in plant cell response to trace metals: polysaccharide remodeling and its role in defense strategy. Acta Physiol Plant. 2011;33.
59. Li T, Zhang Y, Liu Y, Li X, Hao G, Han Q, Dirk L, Downie A, Ruan Y, Wang J, Wang G, Zhao T. Raffinose synthase enhances drought tolerance through raffinose synthesis or galactinol hydrolysis in maize and Arabidopsis plants. J Biol Chem. 2020;295:8064–77.
60. Huo D, Hao Y, Zou J, Qin L, Wang C, Du D. Integrated transcriptome and metabonomic analysis of key metabolic pathways in response to cadmium stress in novel buckwheat and cultivated species. Front Plant Sci. 2023;14.
61. Qin S, Xu Y, Nie Z, Liu H, Gao W, Li C, Zhao P. Metabolomic and antioxidant enzyme activity changes in response to cadmium stress under Boron application of wheat (Triticum aestivum). Environ Sci Pollut Res. 2022;29:34701–13.
62. Gu Q, Xie C, Zhang S, Zhou T, Li N, Xu C, Zhou Z, Wang C, Chen Z. Transcriptomic analysis provides insights into the molecular mechanism of melatonin-mediated cadmium tolerance in *Medicago sativa* L. Ecotoxicol Environ Saf. 2024;278:116411.
63. Li R, Zhou Z, Zhang T, Su H, Li J. Overexpression of *LSU1* and *LSU2* confers cadmium tolerance by manipulating sulfur metabolism in *Arabidopsis*. Chemosphere. 2023;334:139046.
64. Ning H, Zhang C, Yao Y, Yu D. Overexpression of a soybean O-acetylserine (thiol) lyase-encoding gene GmOASTL4 in tobacco increases cysteine levels and enhances tolerance to cadmium stress. Biotechnol Lett. 2010;32:557–64.
65. Zhao M, Xu L, Wang X, Li C, Zhao Y, Cao B, Zhang C, Zhang J, Wang J, Chen Y, Zou G. Microplastics promoted cadmium accumulation in maize plants by improving active cadmium and amino acid synthesis. J Hazard Mater. 2023;447:130788.
66. Fan P, Wu L, Wang Q, Wang Y, Luo H, Song J, Yang M, Yao H, Chen S. Physiological and molecular mechanisms of medicinal plants in response to cadmium stress: current status and future perspective. J Hazard Mater. 2023;450:131008.
67. Yang Z, Yang F, Liu J-L, Wu H-T, Yang H, Shi Y, Liu J, Zhang Y, Luo Y-R, Chen K-M. Heavy metal transporters: functional mechanisms, regulation, and application in phytoremediation. Sci Total Environ. 2022;809:151099.
68. Zhu G, Xiao H, Guo Q, Zhang Z, Zhao J, Yang D. Effects of cadmium stress on growth and amino acid metabolism in two Compositae plants. Ecotoxicol Environ Saf. 2018;158:300–8.
69. Groppa MD, Rosales EP, Iannone MF, Benavides MP. Nitric oxide, polyamines and Cd-induced phytotoxicity in wheat roots. Phytochemistry. 2008;69:2609–15.
70. Nahar K, Hasanuzzaman M, Alam MM, Rahman A, Suzuki T, Fujita M. Polyamine and nitric oxide crosstalk: antagonistic effects on cadmium toxicity in mung bean plants through upregulating the metal detoxification,

antioxidant defense and Methylglyoxal detoxification systems. Ecotoxicol Environ Saf. 2016;126:245–55.
71. Pang B, Zuo D, Yang T, Yu J, Zhou L, Hou Y, Yu J, Ye L, Gu L, Wang H, Du X, Liu Y, Zhu B. *BcaSOD1* enhances cadmium tolerance in Transgenic *Arabidopsis* by regulating the expression of genes related to heavy metal detoxification and arginine synthesis. Plant Physiol Biochem. 2024;206:108299.
72. Li X, Jiang X, Sun J, Zhu C, Li X, Tian L, Liu L, Bai W. Cytoprotective effects of dietary flavonoids against cadmium-induced toxicity. Ann N Y Acad Sci. 2017;1398:5–19.
73. Tohge T, de Souza LP, Fernie AR. Current Understanding of the pathways of flavonoid biosynthesis in model and crop plants. J Exp Bot. 2017;68:4013–28.
74. Yu M, Zhuo R, Lu Z, Li S, Chen J, Wang Y, Li J, Han X. Molecular insights into lignin biosynthesis on cadmium tolerance: morphology, transcriptome and proteome profiling in *Salix matsudana*. J Hazard Mater. 2023;441:129909.
75. Cheng Y, Qiu L, Shen P, Wang Y, Li J, Dai Z, Qi M, Zhou Y, Zou Z. Transcriptome studies on cadmium tolerance and Biochar mitigating cadmium stress in muskmelon. Plant Physiol Biochem. 2023;197:107661.
76. Liu Z-J, Liu X, Zhang Y-L, Guan P, Yang G-L. Physiological and transcriptome characterization provide new sights into cadmium tolerance and accumulation mechanisms in *Tagetes patula* L. Environ Exp Bot. 2024;225:105827.
77. Dong Q, Wu Y, Wang H, Li B, Huang R, Li H, Tao Q, Li Q, Tang X, Xu Q, Luo Y, Wang C. Integrated morphological, physiological and transcriptomic analyses reveal response mechanisms of rice under different cadmium exposure routes. J Hazard Mater. 2024;466:133688.
78. Ma D, Sun D, Wang C, Li Y, Guo T. Expression of flavonoid biosynthesis genes and accumulation of flavonoid in wheat leaves in response to drought stress. Plant Physiol Biochem. 2014;80:60–6.

Publisher's note